Proceedings of the Estonian Academy of Sciences,
2021, **70**, 3, 268–285
https://doi.org/10.3176/proc.2021.3.06
Available online at www.eap.ee/proceedings

MECHATRONICS
AND ELECTRONICS

ADCS development for student CubeSat satellites – TalTech case study

Anton Rassõlkin[a], Toomas Vaimann[a], Peeter Org[b], Alar Leibak[c], Rauno Gordon[d]* and Eiko Priidel[b]

[a] Department of Electrical Power Engineering and Mechatronics, Tallinn University of Technology, 19086 Tallinn, Estonia
[b] Thomas Johann Seebeck Department of Electronics, Tallinn University of Technology, 19086 Tallinn, Estonia
[c] Department of Cybernetics, Tallinn University of Technology, 19086 Tallinn, Estonia
[d] Innovation Centre, Tallinn University of Technology, 19086 Tallinn, Estonia

Received 3 June 2021, accepted 15 June 2021, available online 10 August 2021

Abstract. This paper presents a case study on the development of the Attitude Determination and Control System (ADCS) of Tallinn University of Technology (TalTech) student CubeSat satellites (TTU100 satellite project). To determine the satellite's attitude in orbit and its rotational speed, the satellites are equipped with sun sensors, magnetometers, and gyroscopes. The satellites use magnetorquers and flywheels in 3-axis as actuators to control rotational speed and attitude. The ADCS is used to convert sensor signals into control reference for the actuators. The research focuses on analysing sensors and actuators used in other CubeSat-type satellites as well as on the process of TTU100 hardware and software development. Special attention is paid to selecting software methods for determining the attitude and evaluating the performance of the developed ADCS. The necessity of further study and dissemination of the mission results is suggested.

Key words: small satellites, attitude determination and control, Earth observation, sensor software.

1. INTRODUCTION

TTU100 is a satellite project funded by Tallinn University of Technology to provide students with practical engineering experience. The TTU100 satellite was built according to the CubeSat Program standard [1]. The cube shape with sides of 10 cm and weight below 1.33 kg is the main requirement (characteristic) of a CubeSat-type satellite. This standard was developed in 1999 by California Polytechnic State University and Stanford University to provide access to space for small objects. CubeSat-type satellites are commonly launched as secondary payloads on launch vehicles or put into orbit by deployers on the International Space Station. To ensure the safety and success of the CubeSat Program, satellite developers should play an active role in it by implementing good engineering practices, performing testing, and verifying their systems [1]. The majority of CubeSat missions have been developed in the academic context by students. Due to that fact, the bulk of that type of satellites fail right after the deployment, according to statistical analysis [2]. Failures of some of the CubeSat's satellite subsystems can potentially damage the launch vehicle or a primary payload and put the entire launching of CubeSat Program satellites in jeopardy. Incorrect action may produce space debris that will require additional effort and economic cost to mitigate it. To avoid that, Digital Twins can be used for tracking and detecting satellites that have stopped functioning, as well as for calculating safe trajectories for already operating or new satellites [3]. Special requirements apply to the power systems of CubeSat Program satellites to prevent activating any powered functions during installation and allocation

* Corresponding author, rauno.gordon@taltech.ee

in the launcher tube, called Poly Pico-satellite Orbital Deployer (P-POD), from the time of delivery to the launch vehicle through on-orbit deployment. Power functions of the CubeSat Program satellites include a variety of subsystems, such as deployable mechanism actuation, Command and Data Handling (C&DH), Radio Frequency (RF) Communication, and obviously the Attitude Determination and Control System (ADCS).

The ADCS usually has its processor, sensors, and actuators independent of the rest of the satellite's subsystems. ADCS systems can use various methods for determining attitude, which are most commonly vector observations of particular objects. Different methods are employed for both determining and controlling a satellite's attitude, the most common of which are listed below:

- Sun sensors are popular, accurate and reliable visible-light detectors used to estimate the Sun's direction in the satellite's body reference frame (SBRF). Sun sensors can be quite accurate – 0.01 deg [4], but it is not always possible to take advantage of that feature, e.g. during eclipse. CubeSat projects often use solar panels such as sun sensors – each panel gives a different power output depending on the incident angle of the sun rays, and the sun vector can be reconstructed using trigonometry [5].
- Gyroscope is a spinning wheel, which retains the orientation of its spinning axis due to the conservation of angular momentum. Modern gyroscopes are lightweight and measure angular velocity and acceleration accurately. However, due to axial precession and the fact that the gyroscope does not keep its orientation when not spinning, gyroscopes alone cannot be used to determine a satellite's attitude. Some CubeSat projects have used a low-cost camera assembly and processing hardware as stellar gyroscope [6]. Due to measurements of absolute attitude changes and not angular rates, such a gyroscope can be used to measure attitude changes from a known initial condition without a drift, while sufficient stars are common across frames.
- Magnetic sensors (magnetometers) measure the magnetic field and its strength in three dimensions and therefore return the magnetic field vector [5]. Comparing the magnetic field reading to an onboard Earth's magnetic field model can determine the satellite's attitude. The magnetometer allocation is based on the ADCS design and being placed on the system's printed circuit board (PCB) or an external sensor head. The second option, where the magnetometer placement moves away from the satellite body, is less affected by the magnetic noise inside the satellite [7].
- Star tracker is a camera, mounted on the satellite board, which takes photos of stars and compares them to an onboard model of the night sky to determine the attitude. Star trackers are often the most accurate instruments in ADCS and control systems, but often present a slow update rate, requiring additional sensor and sensor fusion algorithms to provide a smoother and faster output [8]. Furthermore, star trackers need relatively large computational power, which usually means an additional standalone field-programmable gate array (FPGA). They also need the satellite to be still, which means that the star tracker is usually not a very good option for CubeSat projects.
- Earth horizon sensors are usually digital cameras with a fixed focus lens, which takes pictures of the Earth's horizon [9]. The Earth is always bright and not easily confused with other bodies. Infrared (IR) Earth horizon sensors are effective and relatively inexpensive means of attitude determination in the low Earth orbit (LEO) and are well-suited for Earth-observing missions [10] – they are applied in some CubeSat Projects [11].

For attitude control, satellites can use passive methods such as gravity booms or permanent magnets, or active methods such as magnetic coils, reaction wheels, thrusters, or solar sails. One-unit (1U) type satellites mainly use two types of actuators:

- Magnetic coils (magnetorquers) create a magnetic field which will interact with the Earth's magnetic field and create a small external force on the satellite's body.
- Reaction wheels that can be spun to create an internal force on the satellite's body are meant to make quick, sharp changes to the satellite's attitude.

As it can be seen from the nanosatellites' statistics [12], the majority of the satellites (52.5%) are developed by private organizations. However, the share of satellites similar to the TTU100 university project is also high (30.6%). The minority are non-profit organizations (4.6%), space agencies (4.4%), military projects (4.25%), institutes (2.7%), schools (0.8%), and even individual projects from space enthusiasts. Figure 1 confirms the rising interest from the community in such projects and as of April 4, 2021, the number of successfully launched satellites has more than doubled in comparison to the year 2020.

The type and number of sensors and actuators are unique for each satellite. Table 1 presents a configuration of 1U-size satellites' ADCS for academic CubeSat missions, developed by students around the world and launched in recent years. As it can be seen in the table, most of the 1U-size satellites have a similar set of sensors. Usually there are gyroscopes, sun and magnetic sensors. The research work published by universities (presented in Table 1) was analysed and the general configuration of TTU100 was prepared based on the references.

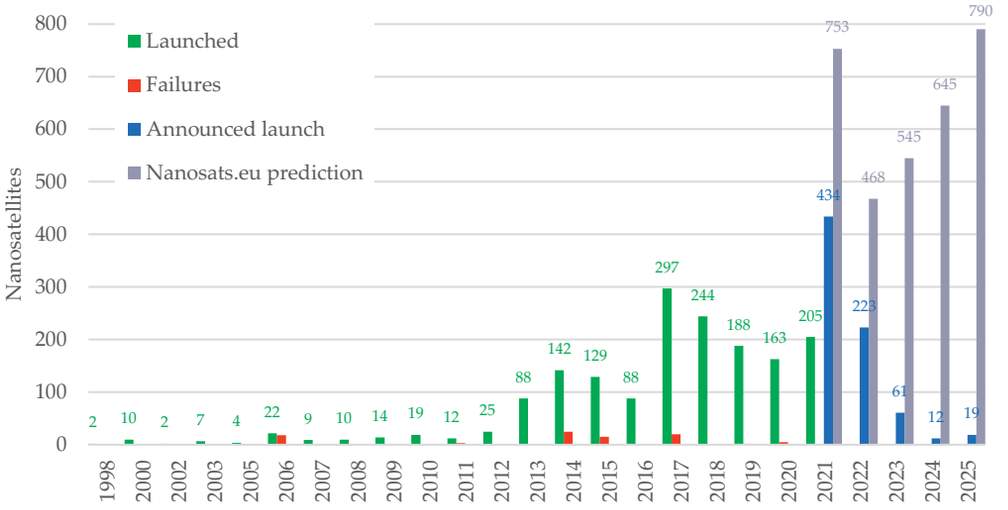

Fig. 1. Nanosatellite launches and forecasts.

Table 1. ADCS configuration of some recently launched 1U academic CubeSat satellites

University (Country)	Satellite	Sensors										Actuators		References
		Accelerometer	Sun sensor	Gyroscope	Magnetic sensor	IR sensor	Star tracker	Horizon sensor	Earth sensor	Temperature sensor	LEO GPS	Magnetorquer (3 pieces)	Reaction wheel (3 pieces)	
Technical University of Denmark (Denmark)	DTUsat		OK		OK							OK		[15]
	DTUsat-2		OK		OK				OK					
Aalborg University (Denmark)	AAUSat-1											OK		[16]
	AAUSat-2		OK	OK	OK							OK	OK	
	AAUSat-3		OK	OK	4					3	OK	9		
Tohoku University and Hokkaido University (Japan)	RISING-2		4	OK			2					OK	OK	[17]
Chinese Academy of Sciences (China)	TZ-1		3		2							OK	OK	[18]
Space Technologies Research Institute (Turkey)	RASAT		4		2		OK				2		OK	[19]
Politecnico di Torino (Italy)	AraMiS		OK	OK	OK							OK	OK	[20]
Consortium of 7 engineering colleges (India)	STUDSAT			3	3							OK		[21]
Tallinn University of Technology (Estonia)	TTU100		OK	OK	OK	OK						OK	OK	

However, Koyuncu et al. in [13] also include micro-pulsed plasma thrusters for experimental purposes. A pulsed plasma thruster is an electromagnetic propulsion system that ablates, ionizes a solid material (normally PTFE, more commonly known as teflon), and then accelerates the plasma with the Lorentz Force to generate thrust [14].

In this paper, the ADCS corresponding to the TTU100 satellite is introduced. A detailed description of the TTU100 satellite is presented in Section 2. In Section 3, a selection of ADCS components is provided and the corresponding installation design is proposed. Section 3 covers a selection of software methods for determining the attitude and evaluation of the developed software's performance. The control requirements for software to implement the operating modes is defined in Section 4. The developed hardware drivers are presented in Section 5.

Section 6 provides an example of determining the location of the Earth with respect to the satellite. Section 7 presents conclusions and suggests future work.

2. TTU100 SATELLITE

Tallinn University of Technology (TalTech) with its Innovation and Business Centre Mektory started a satellite program directed to students and professors in collaboration with engineering and space technology industries from Estonia and other countries. One of the program's missions is to provide a high-quality workforce for high-tech companies in Estonia and other countries. Through the actions of the program, two Student CubeSat satellites with the Estonian names "Koit" and "Hämarik" were sent into orbit (in 2019 and 2020, respectively). The "Hämarik" satellite was the first with which connection was established on November 15, 2020. Its international designator in the database is 2020-061AS, the original name of the object was Object AS and the official name after establishing the connection is TTU100 (the latest location and other detailed information about "Hämarik" can be found at https://www.n2yo.com/satellite/?s=46312).

Connection with the "Koit" satellite was established on November 21, 2020. Its international designation in the database is 2019-038R, the original name of the object was Object R and the official name after establishing the connection is TTU101 (the latest location and other detailed information about "Koit" is available at https://www.n2yo.com/satellite/?s=44401).

The primary mission of the functionally identical satellites is Earth observation using visible light and near-infrared cameras, as well as demonstration of Earth observation technologies. Two radios are utilized for communication with the ground station, one in an ultra-high frequency range for basic two-way communication and the other in an X-band range for downloading larger data, such as images captured by cameras.

In addition to know-how in satellite development, computational fault tolerance and optical communication experiments have been planned. The experiment for fault tolerance of computers will be carried out on a reprogrammable FPGA integrated circuit. Different computer hardware configurations can be implemented in this chip. Space is not too friendly to electronics – the radiation from the Sun can cause bit-flips in computer memory and processors. It can also be permanently damaging in some cases. The bit-flips happen randomly and can cause false results or even crash the system. The faults need to be detected and corrected for electronics to function. It is possible to test different computational hardware configurations to determine the more fault-tolerant systems. This experiment also helps to advance the development of microelectronics on the ground. Today the mission has reached high integration where the low radiation on the ground can already cause bit-flipping in most modern computer chips.

For optical communication experiments, LEDs and laser diodes are on the satellite to transmit signals. On the ground station, it is planned to build a tracking telescope with optical sensors to see the blinking satellite and decode the data. The satellite can turn the LEDs and lasers towards the ground and transmit test signals. The telescope will track the motion of the satellite, and it will be possible to see slow blinking. In this way, data can be sent to the ground from the TTU100 satellite. Different sensor types can be tested, and wavelengths of the LEDs or lasers can transmit data through the atmosphere. The distance between the satellite and the ground station is 500 km in the best case. The most important question to answer is whether it is more effective to transmit data through the atmosphere with coherent light (lasers) or non-coherent light (LEDs).

The TTU100 satellite, shown in Fig. 2, follows the 1U CubeSat standard and uses deployable "wings", which are essentially two extra solar panels (in addition to those mounted on the sides) that would increase battery charging speed if correctly pointed towards the Sun.

The TTU100 satellite requires an ADCS for various mission objectives, mostly for pointing the cameras and X-band radio towards target positions as follows:

1. The system must be able to detumble the satellite from spin rates of ± 50°/s down to ± 0.15°/s (two spins per orbit) within seven days.
2. The pointing accuracy of the system:
   2.1. 45 degrees pointing accuracy is required by the UHF(Ultra High Frequency)-band communication system;
   2.2. 10 degrees pointing accuracy is required by the X-band communication system;
   2.3. 3 degrees pointing accuracy is required by the camera system;
   2.4. 3 degrees pointing accuracy is required by the laser communication experiment.
3. The system must implement remotely configurable parameters for the attitude control loop and readable status for all sensors and control loop states.
4. The system must support remote programming:
   4.1. An incomplete programming sequence must not cause the system to fail to receive a new programming attempt;
   4.2. The software part responsible for checking the health of the leading software image must not be overwritten.

The primary operating modes of the system are defined as follows:

- Detumbling is a process of slowing high rotation speeds after launch, so that standard determination and control algorithms can be switched over;

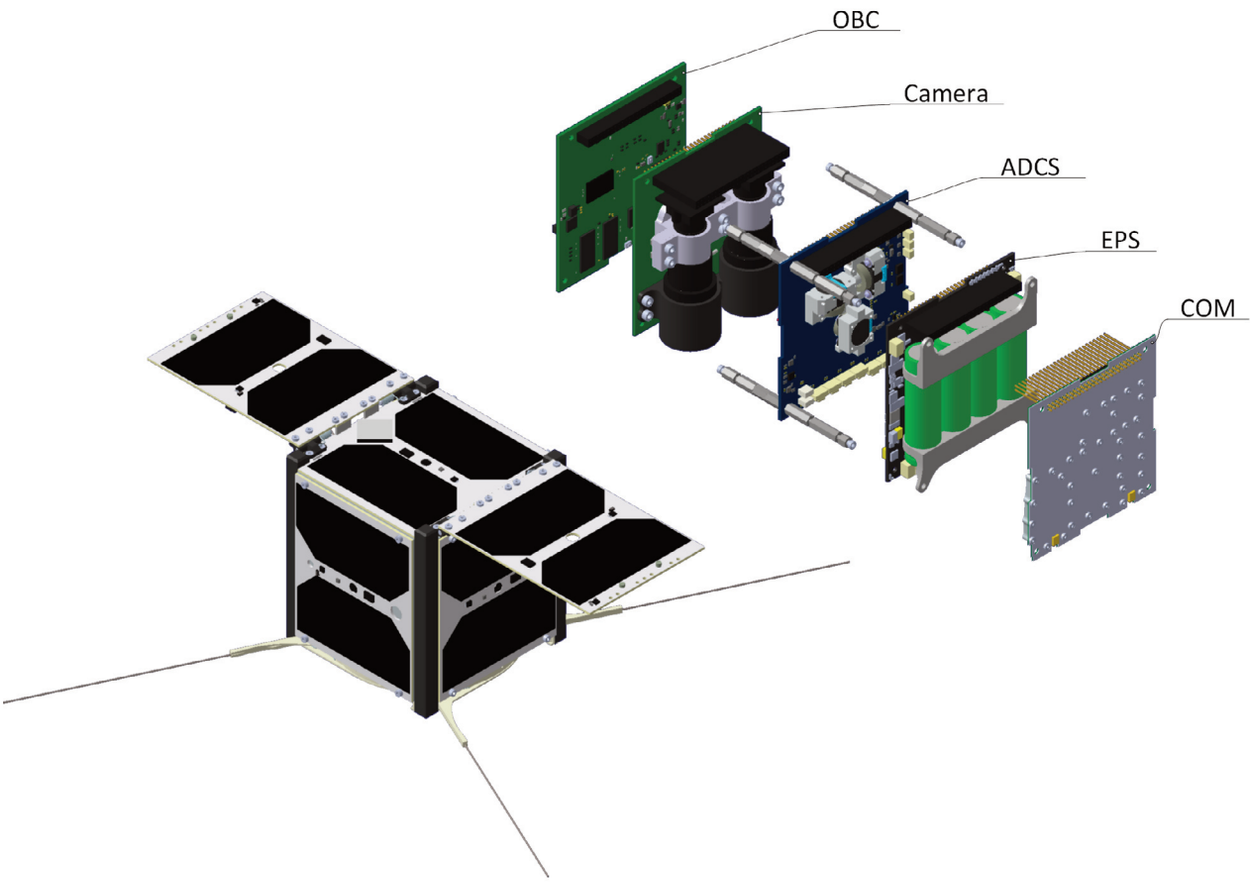

Fig. 2. Representation of the TTU100 satellite and its main components: OBC (On-Board Computer), ADCS (Attitude Determination and Control System), EPS (Electronic Power System), and COM (Communications) boards.

- Y-Thomson spin, according to [1], is a state where the spin axis of the satellite is aligned with the axis of the orbit and spinning frequency is aligned with the frequency of the orbit, keeping one point of the satellite always conveniently pointed towards the Earth;
- Tracking a geographical point on Earth (for image capture);
- Sun pointing (for maximal power harvesting).

According to the requirements presented above and the report by Starin and Eterno [15], the ADCS design steps can be defined as shown in Fig. 3. Steps 1–4 of the ADCS design are primarily covered in the research literature and the current research is focused on Step 5, which is defining the determination and control algorithms as well as developing the software. The research outputs are algorithms and parameters for each determination and control mode, also the modes changing logic. The development process is iterative, the software is developed and evaluated when a design decision is made, and more complicated decisions are made based on the existing software.

3. ADCS DEVELOPMENT

3.1. Hardware

For computation and control tasks, the system uses STM32F303VE, a 32-bit Arm Cortex-M4 based microcontroller unit (MCU) clocked at 72 MHz, with 512 kB of flash storage and 80 kB of RAM. The MCU has a float-point unit, direct memory access capability, and a wide variety of peripherals to work with. The attitude of a satellite is its rotational orientation in space. Moreover, it is also the rotation of its defined body coordinate system in relation to a defined external fixed frame, which is why a mathematical model should represent the attitude before the development of the ADCS [15]. The primary control model is shown in Fig. 4. The ADCS of TTU100 has the following means available for determining attitude: sun sensors to measure the direction of the Sun, magnetometers to measure the direction and strength of the Earth's magnetic field, a gyroscope to measure the rotation speed of the satellite's body, IR sensors to measure the satellite orientation to the Earth. It has the following actuators to

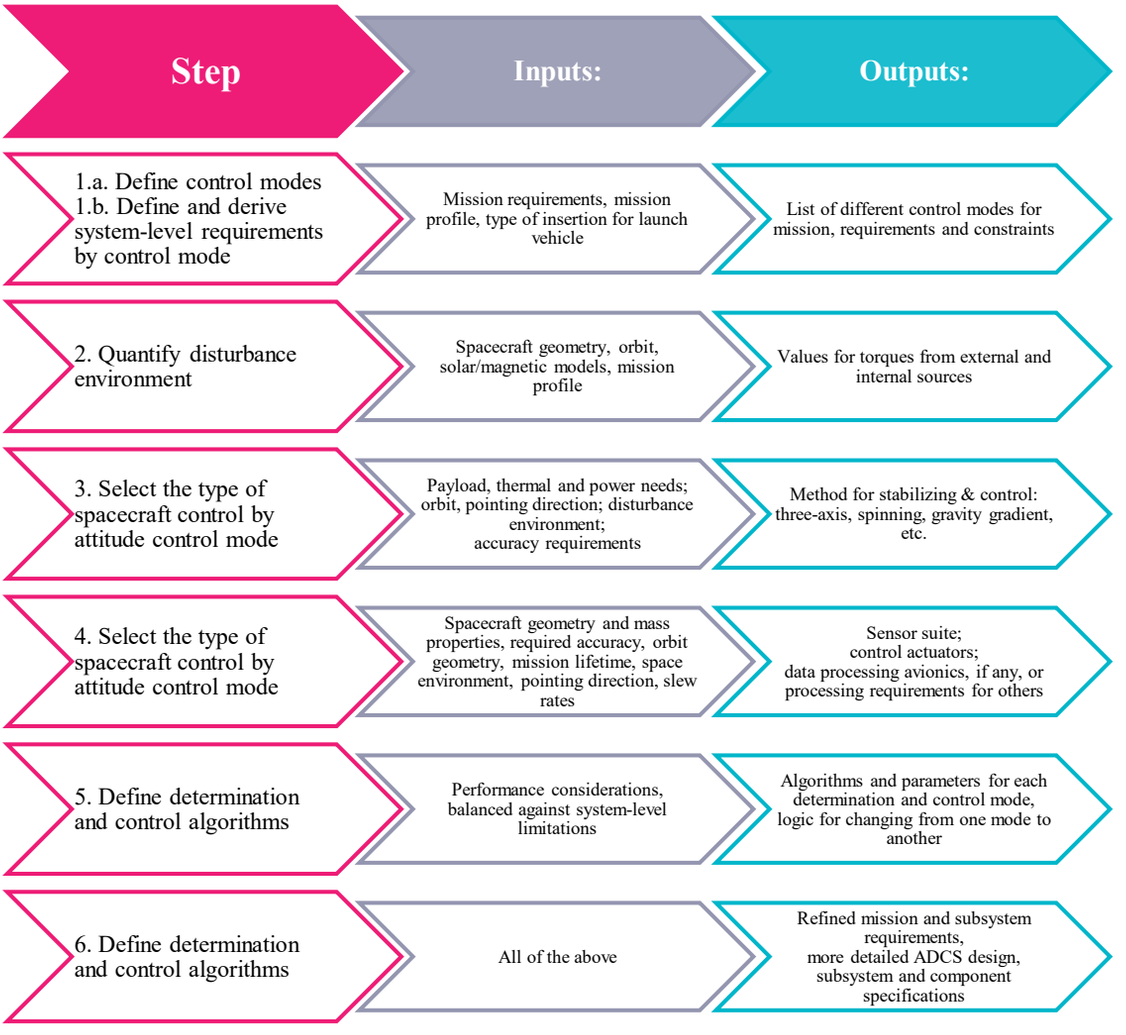

Fig. 3. Design process of an Attitude Determination and Control System (ADCS).

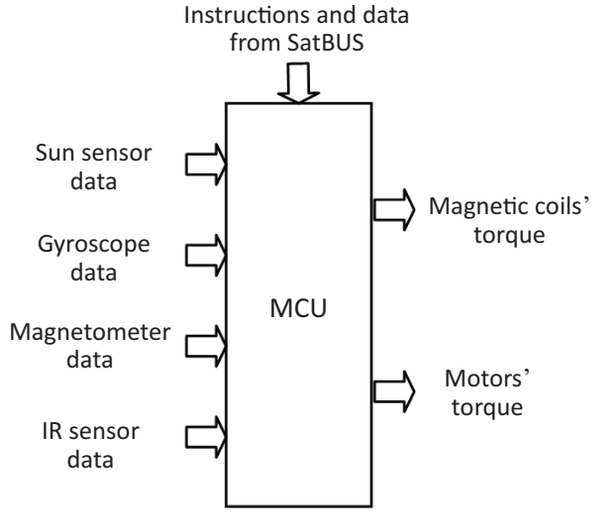

Fig. 4. Basic control model of the developed ADCS.

control attitude: magnetorquers to create a magnetic field which interacts with the Earth's magnetic field and creates a small external force on the satellite's body, and reaction wheels to create an internal force on the satellite's body. Those are meant to make quick, sharp changes to the satellite's attitude. The system has both three magnetic coils and wheels, one for each axis.

For communication with other parts of the satellite, the ADCS is connected to other subsystems via bus (commonly called "satbus") interface following the RS-485 standard. This enables the system to communicate with either the ground station or other subsystems, which are: onboard computer (OBC), communications subsystem (COM), and electrical power system (EPS).

Figure 5 demonstrates the ADCS board with reaction wheels and connectors for coils and visible external sensors. The MCU and most onboard sensors are located on the other side of the board. Losing either magnetometer

Fig. 5. ADCS board.

or gyroscope would result in a mission failure, both sensors are duplicated for redundancy purposes. Magnetorquers are controlled by using digital-analog converters on board the system. For communication between subsystems, the satellite has an RS485 bus. The TTU100 satellite's ADCS uses the STM32F MCU, which is based on the ARM Cortex M4 architecture.

3.2. Determination software and attitude determination methods

Determination software is the most complicated part of the system and uses the most considerable portion of available computation and storage resources. Attitude determination methods fall into two larger categories: spin-axis methods and three-axis methods. The spin-axis methods determine attitude in the form of the axis of spin and angle of rotation, while three-axis methods determine attitude in the three degrees of freedom a spacecraft has in space. Most deterministic attitude determination algorithms are based on finding the optimal solution to the Wahba's problem [22,23].

Spin-axis attitude determination methods are intended for use in spacecrafts which are spin-stabilized [24] and have very few and rudimentary sensors available to work with. Only one sensor is needed for these methods to work, such as a Z-axis magnetometer (Z being the spin axis of the craft), a single-axis sun sensor, or an Earth horizon scanner [25]. The advantages of spin-axis methods are that they require a minimal number of sensors and minimal computing power. The main disadvantage is the requirement of the spacecraft to be spin-stabilized.

The spin-axis attitude determination method used to be common in the 1970s but receives much less attention nowadays [25]. Being completely outdated, it only deserves mention in this research and will not be considered for further study or use in the TalTech satellites. All the other methods covered in this research fall into the category of three-axis attitude determination methods.

The Tri-Axial Attitude Determination (TRIAD) method is the simplest of the three-axis methods, and it takes two 3D unit vector measurements produced by onboard sensors and two unit-vector measurements from known associated reference frames. These can, for example, be the Sun's and the Earth's magnetic fields. The reference vectors can be transformed to the corresponding observed vectors using the (unknown) attitude matrix [24].

The method described by Markley and Mortari in [26] is based on the principle that the desired attitude matrix A can be found from an orthogonal right-handed triad of vectors $\{b_1\ b_2\ b_3\}$ in body frame and $\{r_1\ r_2\ r_3\}$ in reference frame as follows:

$$\begin{aligned} A &= [b_1 \vdots b_2 \vdots b_3][r_1 \vdots r_2 \vdots r_3] \\ &= r_1 b_1^T + r_2 b_2^T + r_3 b_3^T . \end{aligned} \tag{1}$$

Two vectors are provided from measurements and models and the third vector can easily be calculated from the cross product of the two (normalized) vectors:

$$v_3 = \frac{v_1 \times v_2}{|v_1 \times v_2|}. \tag{2}$$

All three vectors must be orthogonal, which in most real situations is not the case. Therefore, one of the two initial vector pairs needs to be "reconstructed" from v_3 and the other vector pair. This results in two equations for finding the attitude matrix, depending on which of the two vector pairs is to be used as the "primary":

$$\begin{aligned} A_1 &= b_1 r_1^T + b_3 r_3^T + (b_1 \times b_3)(r_1 \times r_3)^T , \\ A_2 &= b_2 r_2^T + b_3 r_3^T + (b_2 \times b_3)(r_2 \times r_3)^T . \end{aligned} \tag{3}$$

As an advantage of the TRIAD method, its simplicity and fast computation can be highlighted. On the other hand, disadvantages can be listed as follows: only two measurement vectors can be used; part of the second measurement is simply ignored [24]; measurement (and model) errors need to be ignored. The application of the TRIAD method as a single attitude determination method would result in low accuracy, lack of flexibility (only two vectors), and the result format not being quatern.

The singular value decomposition (SVD) method involves solving the Wahba's problem using singular value decomposition on matrix B [27]:

$$B = \sum_{i=1}^{n} a_i b_i r_i^T , \tag{4}$$

which is given by

$$B = USV^T, \tag{5}$$

where b an r are body and reference frame matrices, a is the set of non-negative weights, U and V represent orthogonal matrices, and $S = dia(s_1, s_2, s_3)$ with $s_1 \geq s_2 \geq s_3 \geq 0$ $s_{1..3}$ are the singular values of B. The SVD method is very robust but requires many computations compared to other methods [27]. Moreover, the output is in the undesirable form of an attitude matrix.

The Davenport's q-method successfully devised a matrix K, which conveniently converts the Wahba's problem to quaternions [28]:

$$K\bar{q}^* = \lambda_{max}\,\bar{q}^*, \tag{6}$$

where λmax is the maximal possible characteristic (eigen) value for the matrix K, and $\bar{q}$ is the unknown attitude quaternion.

$$K = \begin{bmatrix} B + B^T - I \cdot tr[B] & z \\ z^T & tr[B] \end{bmatrix}, \tag{7}$$

where the 3×3 matrix B is described by the equation (9).

$$z = \{b_{23} - b_{32}, b_{31} - b_{13}, b_{12} - b_{21}, \}^T, \tag{8}$$

with b_{xy} being members of the matrix B.

The equation (7) reduces the problem of finding the most considerable characteristic value of K, after which deriving the optimal quaternion is a simple process. This method remains the best method for solving the Wahba's problem, and very robust algorithms exist for eigen decomposition of the matrix K [29]. The original q-method has been superseded by these much faster algorithms listed below.

The Quaternion Estimator (QUEST) finds λ_{max} by applying the Newton-Raphson method to the characteristic polynomial of the matrix K, taking λ_0 as the starting value. λ_0 equals the sum of all weights used to calculate the matrix B, as shown in [30]. The Newton-Raphson method would usually be a very inefficient way to calculate λmax, but in general λ_0 is very close to λ_{max}, which means that the method is able to perform reasonably fast. This is by far the most popular way for satellite attitude determination in spacecrafts [24].

The Estimator of the Optimal Quaternion (ESOQ) and ESOQ2 methods were both devised by Mortari [31,32]. These methods calculate λ_{max} identically using the characteristic polynomial of the matrix K:

$$\begin{gathered} \lambda^4 + b\lambda^2 + c\lambda + d = 0, \\ b = -2(tr[B])^2 + tr[adj(B + B^T)] - z^T z, \\ c = tr\big(adj(K)\big), \\ d = \det(K), \end{gathered} \tag{9}$$

with an auxiliary equation and solution:

$$\begin{gathered} u^3 - bu^2 + 4du + c^2 = 0, \\ u = 2\sqrt{p}cos\left[\frac{1}{3}cos^{-1}\left(\frac{q}{p^{3/2}}\right)\right] + \frac{b}{3}, \end{gathered} \tag{10}$$

where $p = (b/3)^2 + 4d/3$ and $q = (b/3)^3 + \frac{4db}{3} + c^2/2$ and the solution λmax:

$$\lambda_{max} = \frac{\left(\sqrt{u - b} + \sqrt{-u - b - 2\sqrt{u^2 - 4d}}\right)}{2}. \tag{11}$$

Both the ESOQ and ESOQ2 evaluate the associated optimal quaternion by computing the maximum modulus vector cross product among four cross product vectors defined in four-dimensional space. To perform this, the ESOQ implies the computation of seven determinants of 3×3 matrices, while the ESOQ2 reduces the quaternion to the principal axis and angle, reducing the computation to five determinants of 2×2 matrices [32]. The advantages of the ESOQ and ESOQ2 methods can be summarized as follows:

- can have any number of measurement vectors;
- measurement noise is considered (using weights);
- results are in quaternions, which is desirable;
- Q-methods are, however, more complex than the TRIAD.

3.3. Filtering methods

The methods listed above are "single frame" methods, which calculate one deterministic estimation based on one set or frame of measurements, and do not use information about the spacecraft dynamics [26]. A filtering algorithm needs to be added to achieve a more reliable reading containing angular velocities and maybe angular accelerations.

A Kalman filter has been the "workhorse" in many applications. It has also been extensively used in aerospace for decades and been the apparent choice for attitude determination tasks [33]. Such a Kalman filter is called the Linear Kalman Filter (LKF) and it was used for attitude determination in the 1980s due to limitations on onboard processors. Extended Kalman Filters (EKFs) and Unscented Kalman Filters (UKFs) have become more common nowadays, and hardly a satellite exists without one or more onboard [24]. Due to the non-linear nature of the satellite's attitude, using the LKF should be avoided to be able to achieve the best results, whereas the EKF uses non-linear transformation for state transition. The main advantage of the EKF is that it works very well in the case of well-defined state transition models. However, it has a list of disadvantages that can be specified based on Garcia et al. [34]: computationally heavy; challenging

to implement as it needs to derive the Jacobian matrices; limited use cases: transitions need to be differentiable functions; known not to perform very well in a wide variety of situations; known to be outperformed by the UKF in almost every aspect; able to obtain only first-order polynomial accuracy at best.

The UKF was proposed by Julier and Uhlmann in [35]. Most inaccuracy problems of the EKF are caused by the fact that the Gaussian random value (GRV) is propagated through the "first-order" linearization of the non-linear system. The UKF addresses this issue by specifying the GRV through a set of carefully selected points rather than by the mean and covariance matrix. These sigma points are propagated through the non-linear transform and the covariance of the result is approximated from the resulting sigma points [36]. This is called the "unscented transform", and it performs both more accurately and efficiently than the method the EKF uses for predicting the covariance of the result. The advantages of the UKF can be summarized in the following way: obtaining second-order accuracy; rapid implementation, no need to derive Jacobian matrices; the non-linear function can be approached as "black box", meaning that any kind of non-linear transition applies to the UKF.

3.4. Determination algorithm

Since attitude should be represented in quaternion, q-methods are the most desirable. Since these methods are mathematically equivalent, the decision is reduced to the one that is the most efficient, the ESOQ2 [32]. The LKF should not be used for filtering since attitude has non-linear properties. The decision remains between the EKF and the UKF, of which the UKF is known to perform better in every aspect. The final design choice is to use the ESOQ2 in combination with the UKF for attitude determination. The determination flow is shown in Fig. 6.

In most cases where the EKF or the UKF is used for attitude determination, the measurement and reference vectors are passed directly into the filter, and the filter itself performs attitude estimation. Most of the filters fall into the categories of multiplicative or additive EKFs [29]. In the configuration implemented in the TTU100 CubeSat project, the filter is only tasked with removing noise from the estimation of the ESOQ2 and estimating the satellite's other attitude-related states, such as angular velocities and accelerations. The analysis provided by the authors shows several advantages in using this configuration instead, which include:

- The ESOQ2 and other optimal quaternion methods provide an additional output value (e.g. loss function), indicating that the reference vectors' estimation is erroneous, or there are biases in measurement (i.e. if λmax is significantly different from $\lambda 0$).
- Each measurement vector can be assigned with its weights according to their assumed reliabilities; the weights can be changed during the operation and estimated dynamically.
- The measurement vectors and the number of vectors used can be changed without the filter, e.g. sun vector measurement can be exchanged with the Earth's direction from IR sensors when the satellite enters eclipse.
- This configuration has no "first estimation" problem with the filter, which means that the filter can be initialized with the first result from the ESOQ2, and it will be sufficiently accurate.
- The modular structure means more straightforward parametrization and separate components can be reused

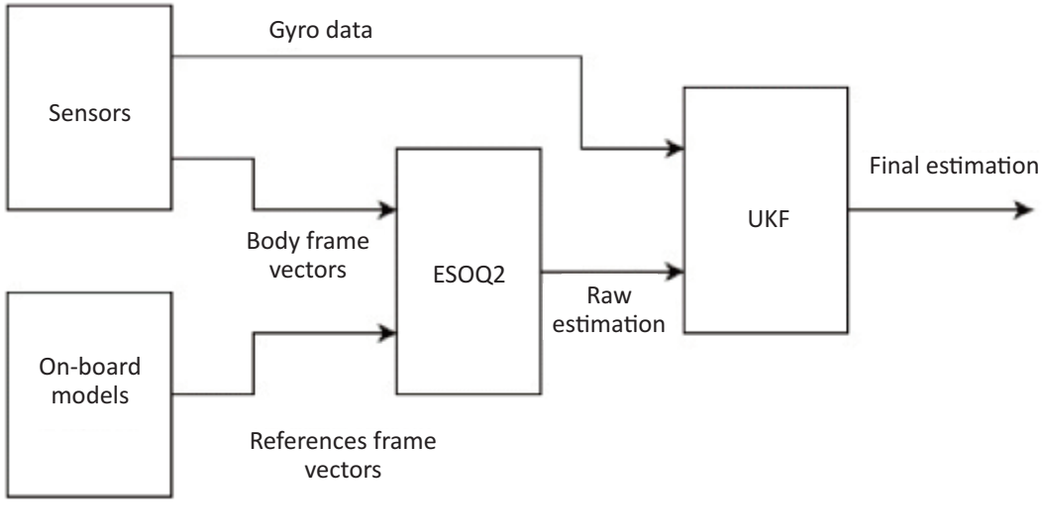

Fig. 6. Attitude determination flow.

in other missions, e.g. the filter could be used for a mission that utilizes a star tracker that already outputs the quaternion from measurement.

The UKF estimates only attitude-related states, estimation of non-attitude states will be performed elsewhere if needed (e.g. sensor biases will be estimated within separate Kalman filters tasked with filtering measurements). The satellite body's moments of inertia will not be estimated at all, as the control algorithm does not use this information as input.

Numerical simulations of the ESOQ2 method show that the correlation between measurement noise and the estimation error is linear. In Fig. 7a, two vector pairs were utilized in the test result, and the angle between the reference vectors was 60 degrees. The figure shows only unfiltered, raw data. When two of the vector pairs, used for attitude calculation, become parallel or antiparallel, calculating attitude in the three degrees of freedom would become mathematically impossible. Therefore, it is expected that there will be an increase in the estimation error as measurement vectors come close to this state. The result of numerical simulation with different angles between measurement vectors is demonstrated in Fig. 7b. In this simulation, a standard noise deviation of 3 degrees was used.

The aforesaid simulation would represent the final accuracy of the ADCS estimation (with static attitude) at 3-degree standard deviation measurement noise if the reference models were 100% accurate (which is an improbable ideal case scenario). The 3-degree standard deviation of the input error was chosen intuitively as the worst case in a real situation. As seen in the graph, even with an average error of 60 degrees, a Kalman filter can reduce the error to around 3 degrees. The sensors will have their own Kalman filters to reduce noise before passing data to the determination algorithm. It means that with similar filtering performance assumed, at 3 degrees of the standard deviation measurement error, the raw measurement error would average around 60 degrees. Noise statistics of the real sensors have not been gathered, but graphical visualization of sensor data has shown the error to be smaller than that.

Those simulations were run with a static attitude. Additional work is required to incorporate state estimation into the filtering to run simulations with a spinning satellite. Those added complexities will inevitably decrease the final estimation accuracy, but even if the final estimation error increased three times, the algorithm's performance would still be adequate, provided that the angle between the measurement vectors remained larger than 4 degrees

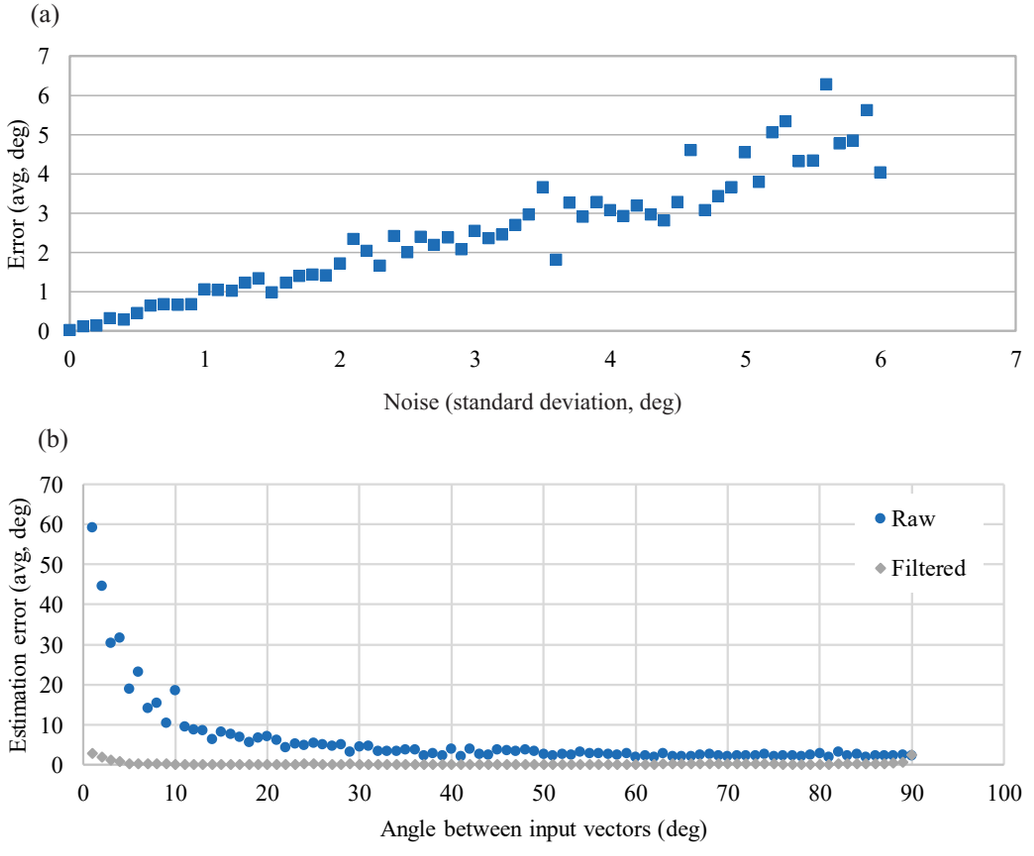

Fig. 7. (a) Attitude error measurement noise and (b) angle dependencies.

(and smaller than 176). Based on numerical simulation results, it is relatively safe to assume that the required accuracy can be reached with the current configuration, given that the accuracy of the models and sensors meets the expectations. Finding this requires actual telemetry returned from the satellite in space.

3.5. Reference models

To provide the reference vectors for the ESOQ2 algorithm, several onboard models are needed. Most of the models require the satellite's position relative to the Earth as input. Several algorithms are available to propagate a satellite's position and the most common of them is SGP4 [22]. This model (like most others available) requires knowing the time (provided by the onboard Real-Time Clock (RTC)) and the orbit model provided by North American Aerospace Defense Command (NORAD) in the form of a two-line element set, uploaded to the satellite and stored in the system's EEPROM. This will need to be updated once every couple of days.

4. CONTROL SOFTWARE

Control software is tasked with implementing the operating modes defined in the requirements. Since the craft's attitude is known, it is evident that attitude control should be performed in the closed loop. State feedback loops use the following system model:

$$\dot{x}(t) = Ax(t) + Bu(t), \tag{12}$$

where $\dot{x}(t)$ is a vector of system states and $u(t)$ denotes the controller input vector, the matrix K must be selected according to

$$u = -Kx, \tag{13}$$

which fulfills the control requirements in a certain way. Several control loops can be created using this model, the example system state being fed back, the system output integral being fed back, or the system state or system error being fed back.

The proportional-integral-derivative (PID) controller is the single most used dynamic control technique, used in 85% of all dynamic controllers [37]. Therefore, it is utilized as the main controller in all control-loop subsystems. As input, the PID takes the target and the actual system state and calculates the error (which would be zero if the target is reached), or simply takes the error as input. The controller can be combined with open-loop components (feed-forward terms), which are functions of the target state instead of the state error. These are useful when the target state needs to maintain the output value. The PID is a simple control technique requiring little knowledge of the systems for implementation. Tuning the controller is also simple and intuitive, and the controller is known to reach the target even when imperfectly tuned, unless it is tuned to be completely unstable. PID parameters are also easy to regulate for more optimized control while the satellite is in space. The PID controller was chosen for all control loops used in the system of the TTU100 satellite. Further development in the controller will include more interesting and suitable examples applicable to this mission, e.g. the linear–quadratic regulator (LQR) [38,39] and model predictive controllers (MPCs) [40,41].

The pointing control loop is shown in Fig. 8. For pointing tasks only the motors are used because magnetorquers would perform hopelessly slow compared to motors to make an impact. Moreover, they interfere with

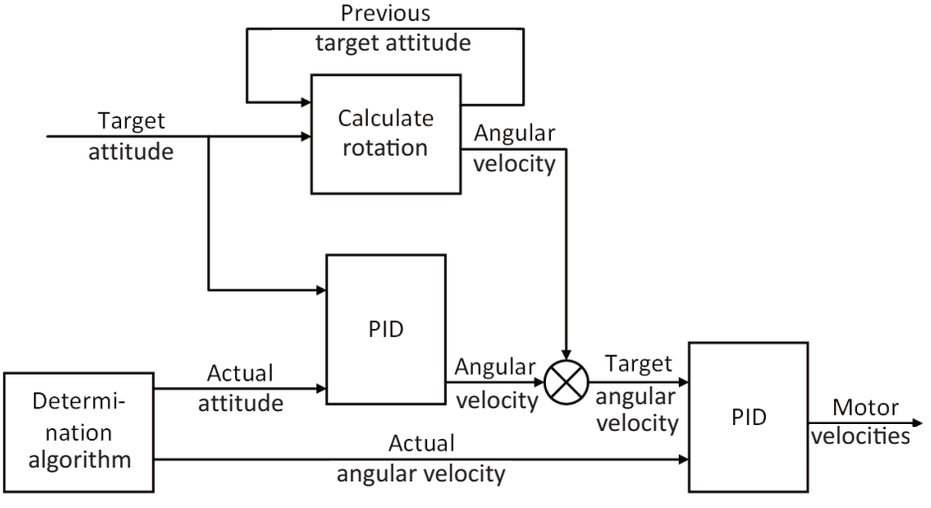

Fig. 8. 3-axis pointing flow.

the magnetic field, making attitude determination difficult. Two separate PID controllers are implemented, one for calculating the satellite's target velocity, taking the target and current attitude as input, and the other for calculating target velocities for the motors, based on the spacecraft's target angular velocity. In most cases, since the satellite is moving in orbit relative to the point of interest, the target attitude also changes in time, which means that the targeted attitude change speed has to be calculated and taken into account as well. All pointing tasks use the same control loop and no separate control algorithm will be implemented for tasks where the target attitude is not going to change significantly (e.g. Sun pointing).

Y-Thomson spin is a convenient state when images need to be captured of the Earth, but rather inconvenient when attempting to point solar panels towards the Sun for charging batteries. This means that depending on the situation, these modes should be switchable. Motors cannot exert an external force on the satellite's body, i.e. constant spin rates would need to be maintained if using motors for switching between those states. This is unwanted because motors should be used sparingly to reduce wear and minimize power consumption. Therefore, only magnetorquers should be used for switching between Y-Thomson spin and standstill. A spin rate controller is implemented for this purpose, which will take the magnetic field, target, and actual spin rates as inputs for magnetorquers accordingly. Only one PID is used for this, which is likely of P variation (without derivative and integral terms), since with only magnetorquers used, the change created in attitude states would take a significant amount of time (measured in hours rather than minutes or seconds), i.e. it is unlikely that derivative and integral terms would make anything useful out of it. This loop cannot be run continuously because magnetic fields created by coils interfere with magnetometer reading, meaning that torque needs to be paused for taking new measurements of the magnetic field and estimating a new attitude. External disturbances on the satellite's body will also be countered by occasionally running this control loop.

After launch, the satellite may be in a fast spin, making communication with a ground station and attitude determination-control either problematic or impossible. To establish proper communication and start using conventional determination and control algorithms, spin rates need to be significantly reduced. Since motors cannot change the satellite's total velocity moments, detumbling needs to be carried out only by means of magnetorquers. To achieve this, the B-Dot control law [42] is used to minimize the magnetic field change. A modified/simplified B-Dot controller is implemented as follows:

$$\begin{aligned} B &= m_k \times m_{k-1}, \\ v &= \frac{B \times m_k}{|B \times m_k|}, \\ g &= 1 - e^{-N \cdot |B|}, \\ T &= v \cdot T_{max} \cdot g, \end{aligned} \tag{14}$$

where T is the output of coils (amount of the current passing through); in the TTU100 case a 3D vector is needed as there are three coils. B represents the change in the magnetic field, m_k and m_{k-l} are current and previous normalized magnetic field measurements, v is the unit vector magnetic field axis to be created by coils, T_{max} denotes the scalar value representing the maximal output of coils, and g is the B-Dot gain. $N \geq 1$ refers to the gain constant. The larger is N, the more torque is applied relative to rotation speed.

This loop is run at around 4 Hz, with most of the time spent on applying torque. Should the frequency be adjusted, the gain constant N should be adjusted accordingly. A tiny delay is needed between releasing the torque and taking a new measurement to let the current in coils and magnetic field around the spacecraft to cool off. This loop will always be run for a specified number of iterations and never in an endless loop for power safety.

5. HARDWARE DRIVERS

Hardware drivers are developed using the firmware library provided by STMicroelectronics, with some exceptions where MCU registers are accessed directly when the performance is critical or the use case is not covered by the firmware library.

Three reaction wheels based on brushless DC (BLDC) motors with an internal Hall effect sensor are used in the TTU100 satellite. The drivers are developed based on the ST's reference manual [30], section 20.3.24. To capture inputs from the Hall sensors, timers in the STM32 have a special mode where Hall sensor inputs are XOR-ed together to detect the change in any of the three inputs. This XOR-ed signal is internally connected to another timer, responsible for creating the pulse weight modulation (PWM) for motor drivers. This timer configuration is referred to as master-slave mode in the ST manual. Change in signal generates commutation interrupt for the timer PWM, which triggers PWM output values from a preloaded register to the output register. For the next commutation event, new values are written in the preloaded registers within the timer's commutation interrupt handler. Using preloaded values and hardware switching means that there is no delay between the new values of Hall sensor update loading, which indicates

maximal efficiency. The motor drivers take target velocity as input, and a PID controller is utilized to adjust the PWM output value based on the target and actual motor velocity. The velocity is measured by means of the capturing timer, and PWM values are updated within the same timer's interrupt handler.

Coil drivers are driven by hardware timers that generate the PWM. Direction is selected using an H-bridge driven by a general-purpose input/output (GPIO). Pins are connected to the MCU so that each coil has its timer associated with them. This design decision was far-sighted because it allows controlling of all the coils with just one timer, such a solution leaves the two other timers free to perform other useful operations.

Most of the sensors for measurement are communicated using simple MCU peripherals such as Inter-Integrated Circuit (I2C) and Serial Peripheral Interface (SPI). The system has six magnetometers available for use, two outside the board on deployable wings and four on the system's board. A large number of sensors is required due to the need to test several different magnetometers in space, and data visualization has shown that magnetometers from different manufacturers could perform very differently. Possible effects on magnetic field measurements have also been an essential factor in designing the satellite's mechanical parts and other subsystems. The magnetometers mounted on the craft's deployable wings will provide a useful comparison to those mounted on the system's board because distortions to the magnetic field will be significantly smaller outside on the wings.

There are eight ambient solar sensors and eight IR sensors, one set for each side and two more for the deployable wings. These sensors are communicated using an I2C peripheral and an I2C multiplexer to handle problems with address conflicts.

Ambient solar sensors have an inherent problem – accuracy becomes low when falling light is already close to 45–60° as small changes around this angle would not result in different amounts of light captured, causing almost no change in reading. To compensate for this, six 18×18 pixel black-white cameras have been installed to determine the Sun's direction more accurately in those areas. These cameras were originally intended for use as mouse sensors and used to capture raw pixel data. To read the data, a serial interface is implemented by bit-banging GPIOs. The clock signal is shared between all the cameras, and for data each has separate GPIOs assigned to them. This means that read operations will not be performed separately for individual cameras but all of the images from the six cameras will be read at once. Unfortunately, the read time is slow, taking around 200–300 ms, which may slow down the determination loop, but in turn, this would give the most reliable measurement vector the available hardware can provide.

There are several other hardware features included in the system, such as a hardware (HW) watchdog, low-frequency (LF) receiver, and high-power light-emitting diode (LED). The HW watchdog is included for additional reliability. This device has a single GPIO as input, and the value needs to be toggled and updated every 1.6 seconds. If this does not happen, the watchdog will switch off the system's power supply for a brief moment. This is being updated in the main loop task if all other tasks respond to pings. A LF receiver – a low-frequency wake-up receiver – is connected to the MCU. This has two inputs, one connected to an unused magnetic coil and the other connected to one of the solar panels. The unused magnetic coil can be employed for a low-frequency radio receiver, and the solar panel can be used for testing visual communication with the satellite. If sufficient light shines on the solar panel, a voltage change will happen – in this way, a high-power laser can be used to send messages to the satellite in space. The unused magnetic coil is also connected directly to an analog pin of the MCU to listen to the input directly. In addition, a high-power LED is connected to the system, which can be utilized to test visual communication with the ground station. The last two hardware features are not related to the system's main goal and serve a scientific purpose. These were added because there were a few more free pins on the MCU. The general structure of the TTU100 satellite's ADCS system is illustrated in Fig. 9.

6. EXAMPLE OF ATTITUDE DETERMINATION

In this example, a possibility for satellite attitude determination by means of sun sensors is presented. First, it is necessary to calculate the sun vector with respect to the satellite's position. The detailed Sun position calculation for the TTU100 satellite is presented in [43]. To verify the calculations, a comparison is made to five different sources: Solar System Calculator (comparing angles; Solar System Calculator by Don Cross available at http://cosinekitty.com/solar_system.html); The Sky Live (ascension, declination, and altitude; The Sky Live Online planetarium can be found at https://theskylive.com/planetarium?obj=sun); Wolfram Alph (comparing angles; to find information in Wolfram, "Sun position in [location] [time]" must be written at https://www.wolframalpha.com); SunCalc (altitude and azimuth; SunCalc available at https://www.suncalc.org/#/59.4364,24.7526,11/2021.04.19/13:56/1/3); Solar Position Algorithm (SPA) (solar zenith and azimuth angles; NREL's Solar Position Algorithm (SPA) can be found at https://midcdmz.nrel.gov/spa). The measurements were made on 2017 May 7 from 15.45 to 16.15 with intervals of 15 min.

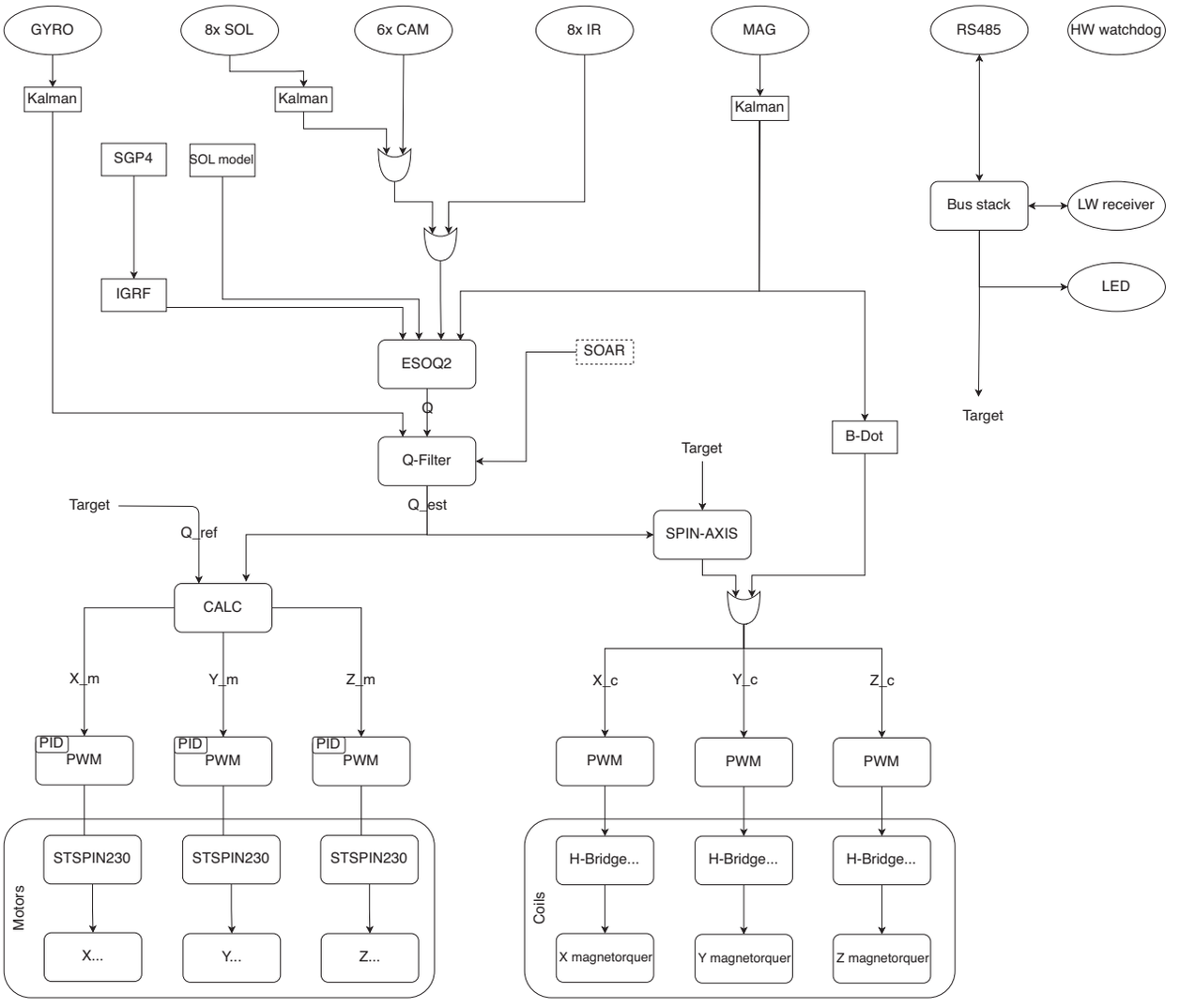

Fig. 9. ADCS diagram of the TTU100 satellite: GYRO – Gyroscope; SGP4 – Simplified perturbations model; IR – Infrared sensor; SOL – Solar sensor; MAG – Magnetic sensor; CAM – Camera; IGRF – International Geomagnetic Reference Field; HW (hardware) watchdog (is an electronic or software timer that is used to detect and recover from computer malfunctions); LW – Longwave (radio receiver); ESOQ2 – Estimator of the optimal quaternion; Q – Quaternion; Q-Filter – Quaternion filter; B-Dot – Detumbling algorithm; SOAR – Satellite Ocean Aerosol Retrieval (algorithm to cover water surfaces).

Figure 10a shows that the result of the Sun determination algorithm (Matlab) taken at 15.45 is about 2.968h. The Solar and Wolfram results are a little less than 2.98h, and the difference with Matlab is 0.012h (0.18°). The SkyLive result is less than that of Matlab (2.963h) and the difference is only 0.005h. Based on that, it can be stated that right ascension calculation is suitable and the algorithm can be used in further calculations. The declination comparison shown in Fig. 10b indicates that the Matlab result is about 16.91° at 15.45. SkyLive gives about 16.882°, Solar 16.958° and Wolfram 16.96°. As seen in the figure, the biggest difference (to Wolfram) is 0.05°and it can be stated that declination is calculated properly. In the altitude angle comparison (Fig. 10c) the Matlab calculation gives the difference of about 2–3°. However, as the altitude changes quickly in one full day, then this difference can be neglected and the result is suitable. The smallest azimuthal angle (Fig. 10d) by Matlab is around 223°, which makes the difference to other sources ca 5–8°. However, as the azimuth changes quickly in one day, then the difference can again be neglected. The difference in right ascension is 0.2%, in declination 0.15%, in altitude 5% and in azimuth 2.5%.

Following that, the calculated vector and the vector from sun sensors must be compared, and after rotating the calculated vector as needed, it is possible to find what the

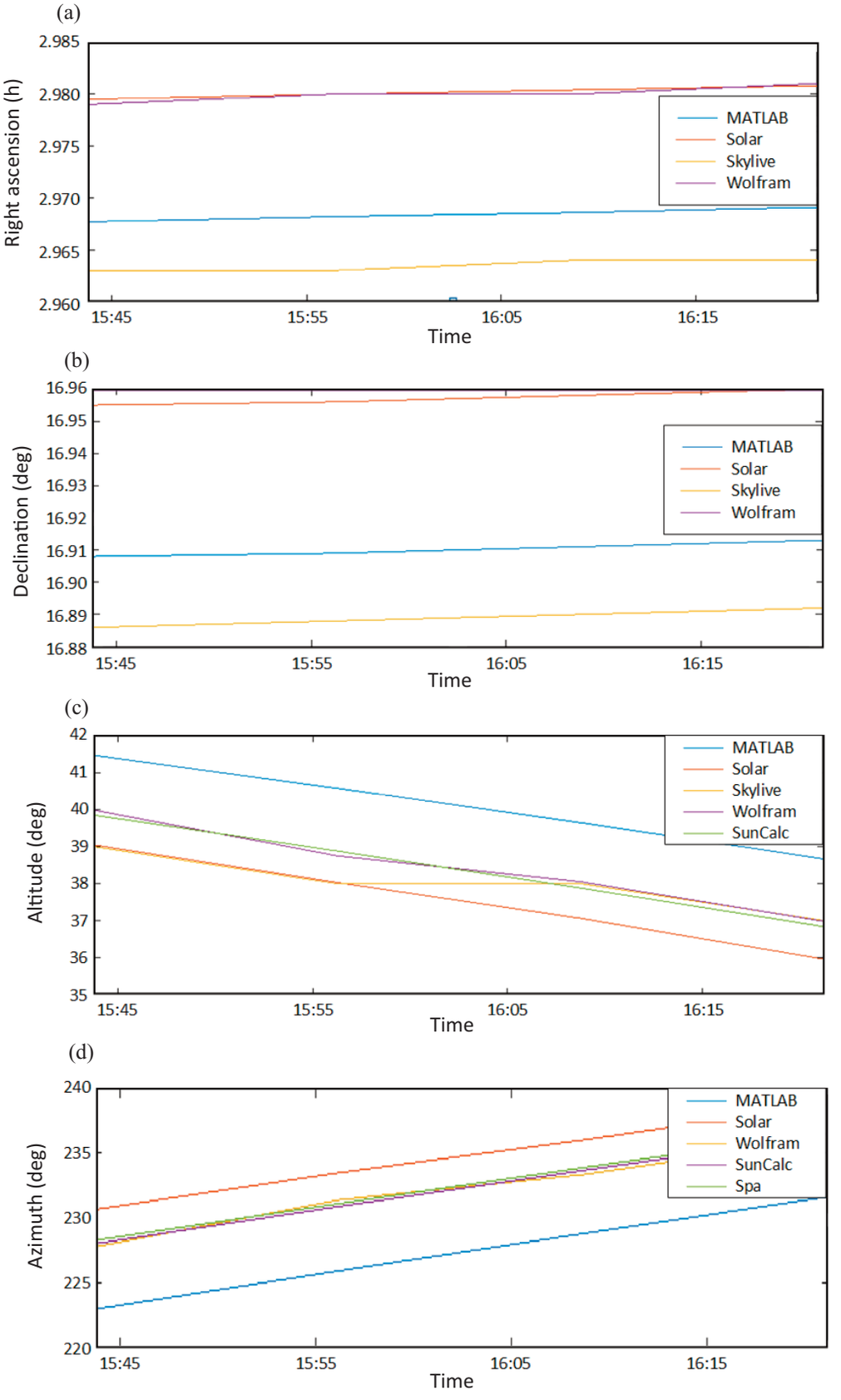

Fig. 10. Sun position algorithm verification by (a) right ascension, (b) declination, (c) altitude and (d) azimuth.

attitude of the satellite is. The program's inputs are timestamp and the satellite's coordinates, and the output is a quaternion representing the rotation. Quaternions are used to rotate the satellite's attitude and to convert the vector from one reference frame to another [44]. Quaternion is the best orientation formation to determine the satellite's attitude because there might be situations where the sunlight does not fall on the satellite as appointed and there might be gimbal lock. Gimbal lock occurs when two axes in the three-dimensional system coincide [45]. It appears in other orientation formations, for example in Euler angles, but not in quaternion. The angle between the calculated (p_1) and sun sensor (p_2) vectors can be found according to

$$\alpha = arccos \frac{p_1 \cdot p_2}{|p_1| \cdot |p_2|}. \quad (15)$$

The cross production between the vectors will be

$$v = p_1 \times p_2 = \begin{pmatrix} \begin{vmatrix} p_1(2) & p_1(3) \\ p_2(2) & p_2(3) \end{vmatrix}, \\ -\begin{vmatrix} p_1(1) & p_1(3) \\ p_2(1) & p_2(3) \end{vmatrix}, \\ \begin{vmatrix} p_1(1) & p_1(1) \\ p_2(1) & p_2(1) \end{vmatrix} \end{pmatrix} \quad (16)$$

and $p_1 \times p_2$ is perpendicular to both vectors. To determinate the required rotational vector, the norm of v must be taken:

$$v = \frac{p_1 \times p_2}{|p_1| \cdot |p_2|}. \quad (17)$$

In this case, the quaternion and its inversion will be calculated based on

$$q = \begin{pmatrix} cos\frac{\alpha}{2} \\ v \cdot sin\frac{\alpha}{2} \end{pmatrix} \text{and } q^{-1} = \begin{pmatrix} cos\frac{\alpha}{2} \\ -v \cdot sin\frac{\alpha}{2} \end{pmatrix}. \quad (18)$$

The rotating angle can be found based on

$$p' = q \cdot p_1 \cdot q^{-1}. \quad (19)$$

When using quaternions in computations, it is important to keep in mind that they are noncommutative, which means that $q \cdot q^{-1} \neq q^{-1} \cdot q$. To receive even more accurate results in the satellite's attitude, the Earth albedo model [4] has to be implemented. It eliminates the sunlight reflected from the Earth.

7. CONCLUSIONS AND FUTURE WORK

Building a satellite is an undertaking that requires multidisciplinary collaboration between mechanical and electrical engineering, mechatronics, electronics, computer systems and software engineers. Thus, participating in such a project helps to develop various important skills such as cross-discipline communication, working on large projects, and understanding large and complex legacy systems. Around 50 students have been involved in various aspects of the satellite development. Integration of the project work into the studies is pursued in two main ways: final theses and project courses. The achievement has been supported by 46 final theses (27 BSc and 19 MSc theses).

The state of the satellites' ACDS software is the following: firmware update is working, tested, and stable; hardware driver development is complete; the system architecture is mostly in place; reference models for the attitude determination are integrated; and most of the determination algorithm is complete and soon ready to be integrated. However, the UKF determination algorithm needs more attention, one-dimensional Kalman Filters currently used for sensor filtering should be replaced with proper filters, preferably the UKF with dual estimation and bias estimation capability. The accuracy of the reference models needs more verification.

A separate study on the effect of the motors mounted directly on the system's board for magnetic field measurement will be conducted. Therefore, telemetry returned from the magnetometers will be an essential scientific outcome of the mission and can form a basis for designing a possible next mission.

Further dissemination of the mission results and the satellites' performance is planned. With the established connection and ongoing mission, results obtained from the orbit as well as comparing simulations and tests with the in-orbit data will be used for further publications.

ACKNOWLEDGEMENTS

The research was supported by Tallinn University of Technology. The publication costs of this article were partially covered by the Estonian Academy of Sciences.

REFERENCES

1. Lee, S., Hutputanasin, A., Toorian, A., Lan, W. and Munakata, R. CubeSat Design Specification Rev. 12. California Polytechnic State University, San Luis Obispo, CA, 2009. https://srl.utu.fi/AuxDOC/tke/radmon/cubesat_standard.pdf (accessed 2021-02-21).
2. Farissi, M. S., Carletta, S. and Nascetti, A. Design and hardware-in-the-loop test of an active magnetic detumbling and pointing control based only on three-axis magnetometer data. In *Proceedings of the 70th International Astronautical Congress, Washington, D. C., USA, October 21–25, 2019*. https://iris.uniroma1.it/handle/11573/1342602#.YN4G1ugzY2w

3. Rassõlkin, A., Orosz, T., Demidova, G. L., Kuts, V., Rjabtšikov, V., Vaimann, T. and Kallaste, A. Implementation of Digital Twins for electrical energy conversion systems in selected case studies. *Proc. Est. Acad. Sci.*, 2021, **70**(1), 19–39. https://doi.org/10.3176/proc.2021.1.03
4. Larson, W. J. and Wertz, J. R. (eds). *Space Mission Analysis and Design.* Third edition. Published jointly by Microcosm Press, El Segundo, CA, and Kluwer Academic Publishers, Dordrecht, 2005.
5. Foletti, A. and Kaewkerd, P. SwissCube Phase A ADCS Report. Technical Report. EFPL Lausanne, 2006.
6. Rawashdeh, S. A., Lumpp, J. E., Barrington-Brown, J. and Pastena, M. A stellar gyroscope for small satellite attitude determination. In *Proceedings of the 26th AIAA/USU Conference on Small Satellites, Logan, UT, USA, August 2012*.
7. Pastena, M. and Barrington, J. Satellite Services Ltd ADCS subsystem for CubeSat: 3-axis high precision control in less than 0.5 U. In *Proceedings of the 1st IAA Conference on University Satellite Mission and CubeSat Workshop in Europe, Rome, Italy, January 24–29, 2011*.
8. Marin, M. and Bang, H. Design and simulation of a high-speed star tracker for direct optical feedback control in ADCS. *Sensors*, 2020, **20**(8). https://doi.org/10.3390/s20082388
9. Daffalla, M. M., Tagelsir, A. and Kajo, A. S. Hardware selection for attitude determination and control subsystem of 1U cube satellite. In *Proceedings of the 2015 International Conference on Computing, Control, Networking, Electronics and Embedded Systems Engineering (ICCNEEE), Khartoum, Sudan, September 7–9, 2015*. IEEE, 2016, 118–122. https://doi.org/10.1109/ICCNEEE.2015.7381441
10. Wertz, J. R. (ed.) *Spacecraft Attitude Determination and Control, vol. 73*. Springer, Dordrecht, 1978.
11. Nguyen, T., Cahoy, K. and Marinan, A. Attitude determination for small satellites with infrared Earth horizon sensors. *J. Spacecr. Rockets*, 2018, **55**(6), 1466–1475. https://doi.org/10.2514/1.A34010
12. Nanosats Database: CubeSat constellations, companies, technologies, missions and more. https://www.nanosats.eu/ (accessed 2021-04-20).
13. Koyuncu, E., Baskaya, E., Cihan, M., Isiksal, S., Fidanoglu, M., Akay, C. et al. ITU-pSAT II: High-precision nanosatellite ADCS development project. In *Proceedings of the 5th International Conference on Recent Advances in Space Technologies – RAST2011, Istanbul, Turkey, June 9–11, 2011.* IEEE, 500–505. https://doi.org/10.1109/RAST.2011.5966887
14. Gatsonis, N. A., Eckman, R., Yin, X., Pencil, E. J. and Myers, R. M. Experimental investigations and numerical modeling of pulsed plasma thruster plumes. *J. Spacecr. Rockets*, 2001, **38**(3), 454–464. https://doi.org/10.2514/2.3704
15. Fléron, R. W. Satellite forensics: Analysing sparse beacon data to reveal the fate of DTUSAT-2. *Int. J. Aerosp. Eng.*, 2019, **2019**. https://doi.org/10.1155/2019/8428167
16. Larsen, J. A. and Nielsen, J. D. Development of cubesats in an educational context – RAST2011. In *Proceedings of the 5th International Conference on Recent Advances in Space Technologies, Istanbul, Turkey, June 9–11, 2011*. IEEE, 777–782. https://doi.org/10.1109/RAST.2011.5966948
17. Liu, Y., Liu, K. P., Li, Y. L., Pan, Q. and Zhang, J. A ground testing system for magnetic-only ADCS of nano-satellites. In *Proceedings of the 2016 IEEE Chinese Guidance, Navigation Control Conference, Nanjing, China, August 12–14, 2016*. IEEE, 2017, 1644–1647. https://doi.org/10.1109/CGNCC.2016.7829037
18. Xia, X., Gao, H., Zhang, K., Xu, W. and Sun, G. ADCS scheme and in-orbit results for TZ-1 satellite. In *Proceedings of the 2020 39th Chinese Control Conference (CCC), Shenyang, China, July 27–29, 2020*. IEEE, 6934–6941. https://doi.org/10.23919/CCC50068.2020.9188513
19. Yavuzyilmaz, Ç., Akbaş, M., Acar, Y., Gulmammadov, F., Kahraman, Ö., Subaşi, Y. et al. Rasat ADCS flight software testing with dynamic attitude simulator environment. In *Proceedings of the 5th International Conference on Recent Advances in Space Technologies – RAST2011, Istanbul, Turkey, June 9–11, 2011*. IEEE, 974–977. https://doi.org/10.1109/RAST.2011.5966987
20. Passerone, C., Reynery, L. M., Iannone, S. and Bonjean, M. The ADCS system in the AraMiS satellite. In *Proceedings of the 2012 IEEE First AESS European Conference on Satellite Telecommunications (ESTEL), Rome, Italy, October 2–5, 2012*. IEEE, 2013, 1–7. https://doi.org/10.1109/ESTEL.2012.6400187
21. Angadi, C., Manjiyani, Z., Dixit, C., Vigneswaran, K., Avinash, G. S., Narendra. P. R. et al. STUDSAT: India's first student Pico-satellite project. In *Proceedings of the 2011 Aerospace Conference, Big Sky, MT, USA, March 5–12, 2011.* IEEE, 1–15. https://doi.org/10.1109/AERO.2011.5747469
22. Wahba, G. A least squares estimate of satellite attitude. *SIAM Rev*., 1965, **7**(3), 409–409. https://doi.org/10.1137/1007077
23. Markley F. L. and Mortari, D. How to estimate attitude from vector observations. 2000, **103**. https://www.researchgate.net/ publication/252610346 (accessed 2021-02-24).
24. van der Ha, J. C. Progress in satellite attitude determination and control. *Aeronaut. Space Sci. Japan*, 2009, **57**(66), 191–198. https://doi.org/10.14822/kjsass.57.666_191
25. Tanygin, S. and Shuster, M. D. Spin-axis attitude estimation. *J. Astronaut. Sci.*, 2007, **55**(1), 107–139. https://doi.org/10.1007/BF03256517
26. Markley, F. L. and Mortari, D. Quaternion attitude estimation using vector observations. *J. Astronaut. Sci.*, 2000, **48**(2–3), 359–380. https://doi.org/10.1007/BF03546284
27. Markley, F. L. Attitude determination using vector observations and the singular value decomposition. *J. Astronaut. Sci.*, 1988, **36**(3), 245–258.
28. Keat, J. E. Analysis of Least-Squares Attitude Determination Routine DOAOP. Computer Sciences Corporation Report CMC/TM-77/6034, 1977.
29. Markley, F. L. and Crassidis, J. L. *Fundamentals of Spacecraft Attitude Determination and Control*. Springer, New York, NY, 2014. https://doi.org/10.1007/978-1-4939-0802-8
30. Shuster, M. D. The quest for better attitudes. *J. Astronaut. Sci*., 2006, **54**(3–4), 657–683. https://doi.org/10.1007/BF03256511
31. Mortari, D. ESOQ: A closed-form solution to the Wahba problem. *J. Astronaut. Sci*., 1997, **45**(2), 195–204. https://doi.org/10.1007/BF03546376
32. Mortari, D. ESOQ-2 single-point algorithm for fast optimal spacecraft attitude determination. In *Proceedings of the Space Flight Mechanics Conference, Huntsville, AL, USA, February 9–12, 1997*. AIAA, 817–826.
33. Kim, Y. and Bang, H. Introduction to Kalman filter and its applications. https://doi.org/10.5772/intechopen.80600

34. Garcia, R. V., Kuga, H. K. and Zanardi, M. C. F. P. S. Unscented Kalman filter for determination of spacecraft attitude using different attitude parameterizations and real data. *J. Aerosp. Technol. Manag*., 2016, **8**(1), 82–90. https://doi.org/10.5028/jatm.v8i1.509
35. Julier, S. J. and Uhlmann, J. K. New extension of the Kalman filter to nonlinear systems. In *Proceedings of SPIE 3068*, *1997*. https://doi.org/10.1117/12.280797
36. Wan, E. A. and Van Der Merwe, R. The unscented Kalman filter for nonlinear estimation. In *Proceedings of the IEEE 2000 Adaptive Systems for Signal Processing, Communications, and Control Symposium, Lake Louise, AB, Canada, October 4, 2000*. IEEE, 2002, 153–158. https://doi.org/10.1109/ASSPCC.2000.882463
37. Paz, R. A. The Design of the PID Controller. New Mexico State University, 2001.
38. Abbas, M. A. and Eklund, J. M. Attitude determination and control sub-system satellite controller. In *Proceedings of the 2011 24th Canadian Conference on Electrical and Computer Engineering (CCECE), Niagara Falls, ON, Canada, May 8–11, 2011*. IEEE, 001440–001445. https://doi.org/10.1109/CCECE.2011.6030701
39. Ure, N. K., Kaya, Y. B. and Inalhan, G. The development of a software and hardware-in-the-loop test system for ITU-PSAT II nano satellite ADCS. In *Proceedings of the 2011 Aerospace Conference, Big Sky, MT, USA, March 5–12, 2011*. IEEE, 1–15. https://doi.org/10.1109/AERO.2011.5747481
40. Krogstad, T. R., Gravdahl, J. T. and Tøndel, P. Explicit model predictive control of a satellite with magnetic torquers. In *Proceedings of the 20th IEEE International Symposium on Intelligent Control, ISIC '05 and the 13th Mediterranean Conference on Control and Automation, MED '05, Limassol, Cyprus, June 27–29, 2005*. IEEE, 2006, **2005**, 491–496. https://doi.org/10.1109/.2005.1467064
41. Chen, X. and Wu, X. Model predictive control of cube satellite with magneto-torquers. In *Proceedings of the 2010 IEEE International Conference on Information and Automation (ICIA), Harbin, China, June 20–23, 2010*. IEEE, 997–1002. https://doi.org/10.1109/ICINFA.2010.5512149
42. Stickler, A. C. and Alfriend, K. T. Elementary magnetic attitude control system. *J. Spacecr. Rockets*, 1976, **13**(5), 282–287. https://doi.org/10.2514/3.57089
43. Pillet, K. Attitude determination of a cube satellite using sun sensors. Bachelor's thesis. Tallinn University of Technology, 2017.
44. Groÿekatthöfer, K. and Yoon, Z. Introduction into quaternions for spacecraft attitude representation. Technical University of Berlin, 2012.
45. Raja, M., Mathur, M., Guven, U. and Prakash, O. Communication and optimization for satellite attitudes using proportional-integral-derivative controller. *International Journal of Scientific Research in Network Security and Communication*, 2019, **7**(6), 1–6.

Asendi määramise ja kontrollsüsteemi arendus kuupsatelliitidele – TalTechi juhtumianalüüs

Anton Rassõlkin, Toomas Vaimann, Peeter Org, Alar Leibak, Rauno Gordon ja Eiko Priidel

On kirjeldatud juhtumianalüüsi asendi määramise ja kontrollsüsteemi arendusest Tallinna Tehnikaülikooli kuupsatelliitidele. Määramaks satelliidi orientatsiooni orbiidil ja selle pöörlemiskiirust, on satelliidid varustatud päikese tajurite, magnetomeetrite ning güroskoopidega. Satelliidid kasutavad kolmes teljes asetsevaid magnettõukureid ja hoorattaid pöörlemiskiiruse ning orientatsiooni juhtimiseks. Asendi määramist ja kontrollsüsteemi kasutatakse tajurite signaalide muundamiseks täiturite juhtsignaalideks. Käesolevas artiklis on kirjeldatud asendi määramise ja kontrollsüsteemi arenduse juhtumianalüüsi TTU100 satelliidile. On keskendutud kuupsatelliitides kasutatavate tajurite ja täiturite analüüsile ning TTU100 satelliidi raud- ja tarkvara arendusele. Tähelepanu on pööratud tarkvara meetodite valikule, et määrata satelliidi orientatsiooni ja hinnata kontrollsüsteemi toimimist. Edasise arenduse ja teavituse vajadus on artiklis välja toodud.